JOURNAL OF CATALYSIS 146, 460–467 (1994)

Formation of Conjugated Iminium Ions from Pyridine on Dealuminated Mazzite

Bich Huong Chiche,* François Fajula,*,[1] and Edoardo Garrone†

*Laboratoire de Chimie Organique Physique et Cinétique Chimique Appliquées, URA 418 CNRS, ENSCM, 8 rue de l'Ecole Normale, 34053 Montpellier Cedex, France; and †Dipartimento di Chimica Inorganica, Chimica Fisica e Chimica dei Materiali, Università di Torino, Via P. Giuria 7, 10125 Torino, Italy

Received March 24, 1993; revised October 15, 1993

High-temperature contact of pyridine with the surface of dealuminated mazzite leads to the appearance of infrared bands at 2914, 2848, 1496, and 1462 cm^{-1}, and to an ultraviolet signal at 205 nm, distinct from those attributable to pyridinium ions and coordinated pyridine. It is proposed that the species responsible for these features correspond to conjugated iminium ions (dihydropyridinium ions) formed by a nucleophilic attack and protonation of pyridine molecules adsorbed on Lewis sites. Their formation would then involve the participation of strong Lewis/Brønsted pairs of sites that could correspond to the superacid site often invoked in zeolitic materials. © 1994 Academic Press, Inc.

INTRODUCTION

Since the pioneering work of Parry (1) in the early sixties, infrared spectroscopy of adsorbed pyridine has been widely and routinely used to probe the nature of the acid sites on the surfaces of solid catalysts. Direct assessment of the acid character, Brønsted or Lewis, of the sites may be gained from the frequency of the 19*b* vibration mode of the adsorbed molecule. The band, which appears at 1440 cm^{-1} in liquid-like or physically adsorbed pyridine, shifts to 1450 cm^{-1} upon formation of coordinated species by adsorption on Lewis sites, and to 1550 cm^{-1} upon formation of pyridinium ions by protonation at Brønsted sites. In most cases, both signals are observed simultaneously, allowing for quantitative evaluation of the ratio between the two types of acidities. Besides the 19*b* frequency, the other vibrational mode sensitive to the state of the probe molecule is the 8*a* one, which can provide further confirmation of the assignments (2, 3).

Analysis of literature data suggests that the position of the pyridinium ion band depends little on the strength of the Brønsted acid sites. By contrast, several studies on the characterization of the acidity of zeolites (4–9) point out that pyridine desorption by high-temperature treatment results in some dehydroxylation of the surface, generating new Lewis sites on which the probe molecule readsorbs. This phenomenon would lead to the development of a new signal, at 1460 ± 3 cm^{-1}, which coexists with the 1450 cm^{-1} one. The reason for the different absorption positions could be a different location and/or a greater strength of the newly created sites, as compared to those of the original ones (9). Recently, however, another interpretation has been proposed to explain the 1460 cm^{-1} signal, namely a decomposition of the probe molecule (10).

Infrared bands at 1460 and 1540 cm^{-1} have also been reported to form after addition of pyridine to solid superacid catalysts (11, 12). They were assigned to coordinated pyridine and pyridinium ions, respectively. After desorption at 573 K, the 1540 cm^{-1} signal disappeared, whereas the absorption band for the Lewis sites was still present, indicating a higher acid strength for the latter sites. Moreover, it was suggested (12) that the sites retaining pyridine above 573 K were the active centres for the isomerization and cracking of light alkanes.

We report here on new infrared and ultraviolet data obtained on steam-dealuminated mazzite zeolite that may question the previous assignation of the 1460 cm^{-1} signal. Several kinds of experimental evidence lead, in fact, to the hypothesis that it could characterize conjugated iminium species resulting from the rearrangement of pyridinium ions on strong Lewis/Brønsted paired sites.

EXPERIMENTAL

Materials

The zeolite samples have been prepared at the Elf Research Centre, in Solaize, by steam dealumination at 923 K for 30 min, under 100% steam, of a parent mazzite (Si/Al = 3.2) synthesized in the presence of tetraethylammonium and sodium cations (13, 14). The silicon-to-aluminium ratio of the framework of the steamed zeolite, determined by using ^{29}Si NMR spectroscopy and infrared

[1] To whom correspondence should be addressed.

0021-9517/94 $6.00

spectroscopy of lattice vibrations (15, 16) was equal to 20 ± 2. Separate portions of this material were acid leached with 0.5, 1, and 1.5 *M* solutions of HNO_3 in order to yield samples with global Si/Al ratios (measured by elemental analysis) of 9, 14, and 20, respectively. It was checked that the acid treatment did not modify the framework Si/Al ratio. In the following, the three samples are referred to as MAZ (20–9), MAZ (20–14), and MAZ (20–20).

Infrared Spectroscopy

The self-supporting wafers (2 cm^2, 20 mg) of zeolite were placed into a quartz IR cell and activated under vacuum (up to 10^{-6} Torr) at 773 K for 10 h. After cooling to 423 K, the cell was equilibrated with 2 Torr of pyridine (spectroscopic grade, dried over Linde 4A molecular sieve and further outgassed by standard freeze–pump–thaw technique) for 12 h. The cell was then evacuated to 10^{-5} Torr to remove the gaseous and weakly adsorbed pyridine. The desorption was then continued at increasing temperatures (2 h plateaux at 573 and 723 K). Infrared spectra were recorded, at room temperature, at each stage of the treatment with a FTIR Nicolet 320 spectrometer (resolution 2 cm^{-1}). *In situ* deuteration of the hydroxyl groups of sample MAZ (20–14) was achieved by contacting the zeolite wafer twice with 10 Torr of deuterium oxide (99.5% isotopic purity) at 523 K for 10 h, then evacuating the cell for 5 h at 523 K and for 6 h at 773 K and, ultimately, cooling to 423 K.

Ultraviolet Spectroscopy

The very same procedure of pyridine adsorption/desorption described above has been followed for the UV study of sample MAZ (20–14). The UV diffuse reflectance (DR) spectra have been recorded at room temperature with a Cary 5 Varian spectrophotometer, equipped with the diffuse reflectance accessory, and processed to obtain the plots of the Kubelka–Munk function, $F(R) = (1 - R)^2/2R$ versus wavelength. The spectral zone 200–500 nm was recorded with a signal averaging time of 0.033 s, a data interval of 1 s, and a scan rate of 1800 nm/min. The zeolite was closely packed in a double-wall fused-quartz cell of 1 mm thickness.

RESULTS

Infrared Spectra of Adsorbed Pyridine

The result of the adsorption of pyridine on the infrared spectrum of dealuminated mazzite is summarized in Fig. 1, where the relevant spectral zones, recorded for MAZ (20–14), are reported. The 2800–3300 cm^{-1} and 1400–1700 cm^{-1} regions are presented, on a different scale, in Figs. 2 and 3, respectively. The effect of the steam and acid leaching treatments on the infrared spectrum of the hydroxyl stretching region (3800–3500 cm^{-1}) of mazzite has been discussed in detail elsewhere (15). The three main features of the spectra originate from isolated silanol groups (peak at 3745 ± 5 cm^{-1}), structural acidic O–H groups (peak at 3610 ± 10 cm^{-1}), and hydrogen-bonded O–H groups (broad band in the range 3700–3300 cm^{-1}).

Pyridine adsorption at 423 K followed by evacuation caused a decrease of the intensity not only of the structural Al–OH–Si hydroxyl groups but also of the silanol groups. This agrees with recent results showing that the SiOH groups were perturbed indirectly by chemisorbed pyridine (17). Note that the various OH stretching vibrations were

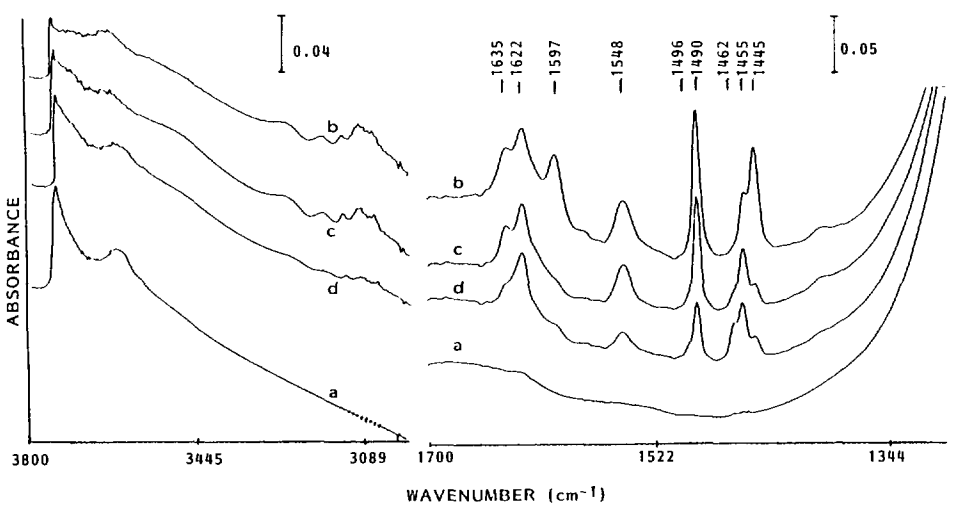

FIG. 1. Infrared spectra of pyridine adsorbed on MAZ (20–14). Starting material outgassed (a) at 773 K, (b) after adsorption of pyridine at 423 K and desorption at 423 K, (c) after desorption at 573 K, and (d) after desorption at 723 K.

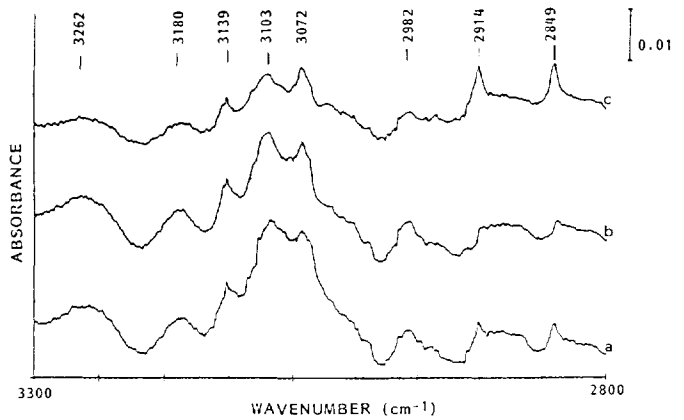

FIG. 2. Infrared spectra of pyridine adsorbed on MAZ (20–14) in the region of the C–H and N–H stretching vibrations (a) after adsorption of pyridine at 423 K and desorption at 423 K, (b) after desorption at 573 K, and (c) after desorption at 723 K.

still discernable, indicating that the whole structure was not accessible to the base. The signals due to chemisorbed pyridine appeared in the region 2800–3300 cm^{-1} for the N–H and C–H stretching vibrations (Fig. 2), and in the region 1400–1700 cm^{-1} for the ring vibrations (Fig. 3). The latter spectral zone also provided evidence for the presence of labile hydrogen-bonded or sodium-bonded species, characterized by absorption bands at 1597 cm^{-1} (8*a* mode) and 1445 cm^{-1} (19*b* mode). In view of the very low sodium content of the samples (<0.1 wt.%) the former species seem more likely. The formation of pyridinium ions was indicated by the bands at 1635 and 1548 cm^{-1}, and the presence of species coordinated to Lewis sites by the signals at 1622 and 1455 cm^{-1} for the 8*a* and 19*b* modes, respectively. The signal at 1490 cm^{-1} is common to both types of species. Besides the aromatic C–H and N–H vibrations, which appear at frequencies above 3000 cm^{-1} (the two bands at 3265 and 3180 cm^{-1} are typical of pyridinium ions), the bond stretching region revealed a doublet at 2914 and 2849 cm^{-1}, characteristic of symmetric and asymmetric saturated C–H stretching vibrations, respectively (Fig. 2), and a signal at 2982 cm^{-1} corresponding to the overtone vibration of the 1490 cm^{-1} peak.

The desorption of pyridine at 573 K led to a decrease of the signals of the hydrogen-bonded species (Fig. 3c), whereas those characterizing pyridine chemisorbed on Brønsted and Lewis sites were hardly affected. Nevertheless, a new signal, appearing as a shoulder at 1462 ± 2 cm^{-1}, became clearly visible. Upon further increasing the desorption temperature, to 723 K (Fig. 3c), this new band grew and became well resolved at 1463 cm^{-1}, and shoulders at 1600 and 1496 cm^{-1} developed. The growth of these signals occurred at the sole expense of the pyridinium species. In the high-frequency zone, all the signals above 3000 cm^{-1} decreased in intensity, whereas that of the doublet at 2914 and 2849 cm^{-1} increased significantly.

Influence of the Extra-Framework Aluminium Content

The influence of the content of extra-framework aluminium on the infrared spectra of adsorbed pyridine has been investigated by performing a study parallel to that reported above on MAZ (20–14), which contains 1.7 framework Al (FAL) per unit cell and 0.7 extra-framework Al (EFAL), on MAZ (20–9) (1.7 FAL and 1.9 EFAL) and MAZ (20–20) (1.7 FAL and no EFAL detected). The results are summarized in Figs. 4 and 5. After pyridine adsorption and evacuation at 423 K the spectra revealed the very same features as above, characteristic of H-bonded pyridine, pyridinium ions, and coordinated pyridine. Direct comparison of the acidity of the three samples on a quantitative basis is hazardous since not all acid centers in the structure are reached by the probe molecule (see above).

Desorption at 573 K eliminated most of the labile species (curves b in Figs. 4 and 5) as well as a significant portion of the chemisorbed pyridine in the case of MAZ (20–20). Pyridine was no longer detected on the latter material after desorption at 723 K (Fig. 5c). A similar treatment of sample MAZ (20–9) led to a decrease of the

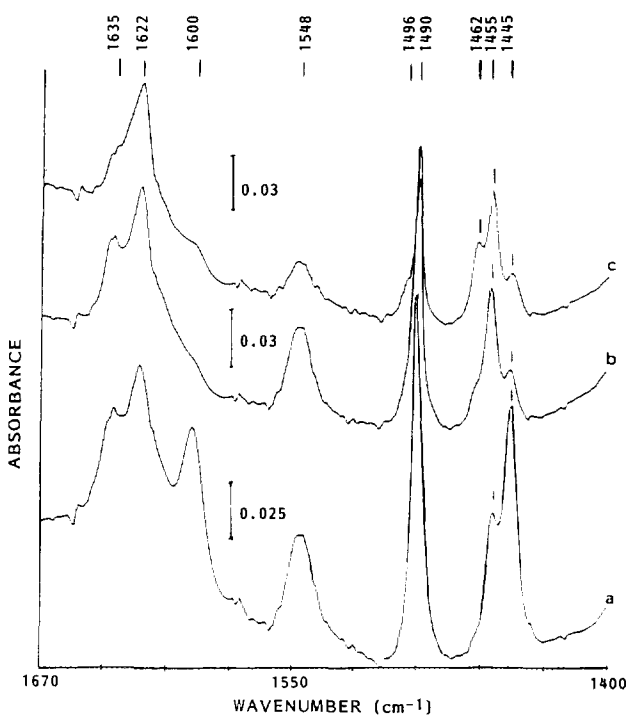

FIG. 3. Infrared spectra of pyridine adsorbed on MAZ (20–14) in the region of the ring vibrations (a) after adsorption of pyridine at 423 K and desorption at 423 K, (b) after desorption at 573 K, and (c) after desorption at 723 K.

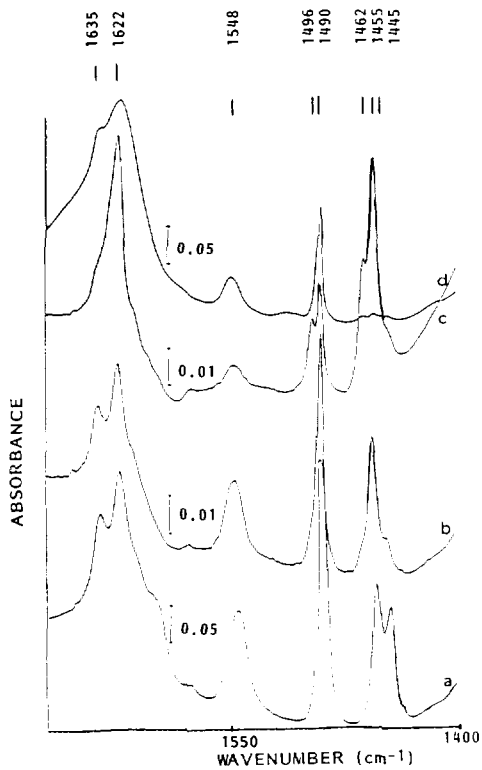

FIG. 4. Infrared spectra of pyridine adsorbed on MAZ (20–9) in the region of the ring vibrations (a) after adsorption of pyridine at 423 K and desorption at 423 K, (b) after desorption at 573 K, (c) after desorption at 723 K, and (d) after rehydration.

intensity of the signals at 1548 and 1635 cm^{-1} associated with pyridinium species and to the development of new bands at 1462 and 1496 cm^{-1} (Fig. 4c). The latter band was much more resolved than on MAZ (20–14). The evolution of the spectral zone of MAZ (20–9) corresponding to the C–H and N–H stretching vibrations, between 2800 and 3300 cm^{-1} (not shown), was comparable to the one reported for MAZ (20–14) in Fig. 2. After desorption at 723 K all the signals above 3000 cm^{-1} decreased in intensity, whereas the doublet at 2914 and 2849 cm^{-1} became the most intense feature of the spectrum.

Effect of Sample Rehydration

In order to verify whether the signals emerging after high-temperature treatment of the zeolite were due to some decomposition of the chemisorbed pyridine, as postulated recently (10), the reversibility of the phenomenon was checked by rehydrating, *in situ*, the pyridine/MAZ (20–9) sample previously desorbed at 723 K. Rehydration was achieved by contacting the sample with ambient atmosphere for 2 min at room temperature, then heating to 723 K, without evacuation, for 2 h. The result of this treatment is shown in Fig. 4d. It is clear that rehydration transformed Lewis sites into Brønsted sites (the intense signal at 1620 cm^{-1} is due to the bending vibration of water molecules) and destroyed the bands at 1462, 1496, 2914, and 2849 cm^{-1}. The formation of carbonaceous species can then be reasonably ruled out to account for the new signals in the spectrum of adsorbed pyridine.

Adsorption of Pyridine on Deuterated MAZ (20–14)

The formation of saturated C–H bonds can be ascertained by infrared spectroscopy using deuteration experiments.

Figure 6a shows the infrared spectrum of pyridine adsorbed on deuterated MAZ (20–14) after 2 h of treatment under vacuum at 723 K. Besides the usual signals already discussed above, the spectrum revealed a weak band at 1437 cm^{-1}. The sample was then reheated to 723 K and maintained at this temperature for 12 h without pumping. The new spectrum recorded after such a treatment (Fig. 6b) showed an increase of the intensity of the 1437 cm^{-1} signal at the expense of the one at 1462 cm^{-1}. Such a change would support the assignment of the latter band to the bending vibration mode of CH_2 groups. The 25 cm^{-1} shift towards lower frequency upon deuteration of the surface would be consistent with the formation of CHD groups. The corresponding C–D stretching modes could not be observed in the 1800–2200 cm^{-1} range. We ascribe this, on the one hand, to the intrinsic intensity of these vibrational modes, which is known to be small, and, on the other hand, to the fact that strong absorption by the zeolite lattice occurs in this region.

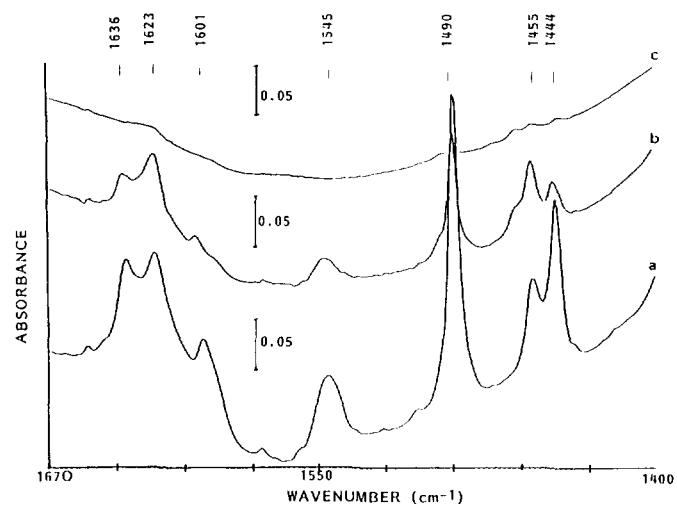

FIG. 5. Infrared spectra of pyridine adsorbed on MAZ (20–20) in the region of the ring vibrations (a) after adsorption of pyridine at 423 K and desorption at 423 K, (b) after desorption at 573 K, and (c) after desorption at 723 K.

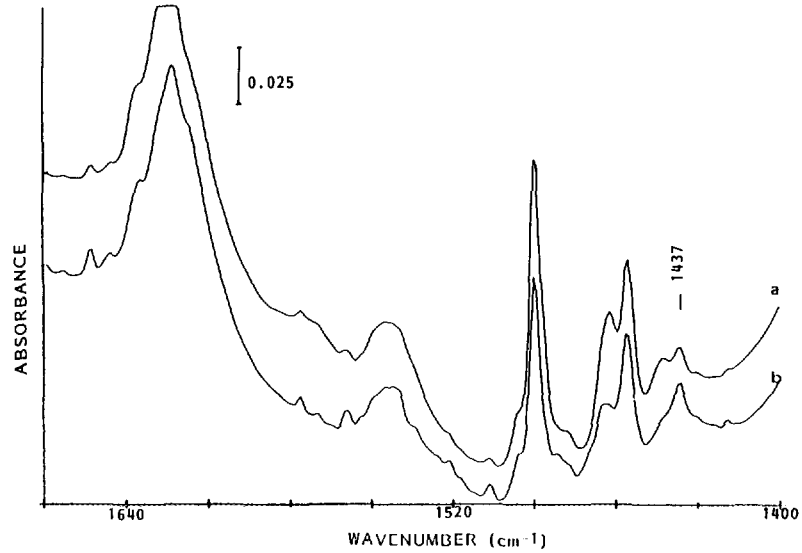

FIG. 6. Infrared spectra of pyridine adsorbed on deuterated MAZ (20–14) (a) after outgassing for 2 h at 723 K and (b) after treatment at 723 K for 12 hours.

UV Spectroscopy of Adsorbed Pyridine

The UV/DR spectrum of the sample after adsorption and desorption of pyridine at 423 K exhibited a very strong band centered around 200 nm and a weaker one centered at 250 nm (Fig. 7b), characteristic of the primary band (λ_{max} = 195 nm) and the fine-structure band (λ_{max} = 250 nm), respectively, of the aromatic ring in pyridine and pyridinium species (18, 19). Upon increasing the desorption temperature (Fig. 7c), the intensity of the first signal decreased significantly, whereas the second band narrowed and the maximum was shifted towards longer wavelength. After desorption at 723 K, the most intense feature of the spectrum appeared at 255 nm, and a second maximum became visible at 205 nm (Fig. 7d). The weak intensity of the 205 nm band, compared to that at 255 nm, rules out its assignment to the primary band of pyridine species. The latter is probably shifted towards a shorter wavelength range, outside the limit acceptable due to the absorption of air in the instrument. Note that the development of the new UV/DR band at 205 nm coincides with the appearance of the signals at 1496 and 1462 cm^{-1} in the infrared spectra. The two phenomena must therefore be related. A UV band at 205 nm characterizes conjugated double bonds (20) and argues in favour of the loss of the aromatic character of part of the adsorbed species. Considering the system under study, we ascribe it to a conjugated iminium (dihydropyridinium) species.

DISCUSSION

The emergence of an infrared band around 1462 cm^{-1} as the temperature of desorption of pyridine from the surface of zeolites is increased has generally been ascribed to the formation of a new pyridine-Lewis site. The latter would be generated either by migration of pyridine from Brønsted sites to vacant Lewis sites (5), by desorption of pyridine from weaker Lewis sites (5), or by dehydroxyla-

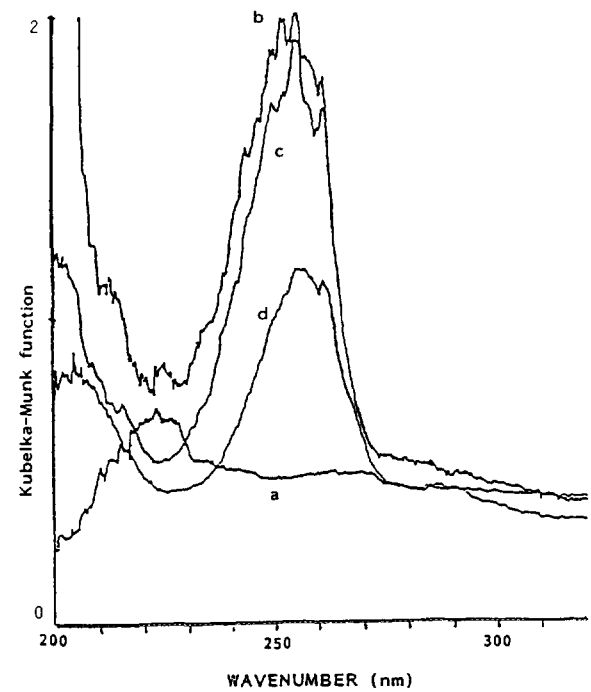

FIG. 7. UV/diffuse reflectance spectra of pyridine adsorbed on MAZ (20–14). Starting material outgassed (a) at 773 K, (b) after adsorption of pyridine at 423 K and desorption at 423 K, (c) after desorption at 573 K, and (d) after desorption at 723 K.

tion of the surface (7–9), this process being enhanced by pyridine desorption (6). In all cases, it is well agreed that these new sites are stronger than the original ones. The general behaviour reported here agrees, to some extent, with the above conclusions. The new species develop at the sole expense of the pyridinium ions, they are adsorbed strongly on the surface but disappear upon rehydration, and their formation is favoured by the presence of extra-framework species. All these facts support then the hypothesis that Lewis centres are involved in the adsorption process. Our data nevertheless provide several pieces of evidence that make the assignment of the 1462 cm^{-1} signal to a different kind of coordinated pyridine or to decomposition products unlikely. First, its behaviour upon deuteration suggests that it is due to a C–H bending vibration mode rather than to a C=C stretching one. Second, concomitant with the growth of the 1462 cm^{-1} signal, a doublet, at 2914 and 2848 cm^{-1}, characteristic of C–H stretching vibrations in aliphatic CH_2 groups, develops, suggesting a progressive loss of the aromatic character of the pyridine ring. Third, the loss of aromaticity is confirmed by the UV/DR data, which demonstrate the formation of a conjugated imine form at high temperature. Note that the infrared bands at 1600 and 1496 cm^{-1} can also be attributed to a nitrogen-containing conjugated system. Signals at 1595 and 1495 cm^{-1} appear in the spectrum of pyrrole adsorbed on acidic surfaces, and have been assigned to species held on Lewis sites (21). Finally, rehydration of the zeolite restores the original spectrum, ruling out a decomposition of the base molecule.

In order to take into account all the above observations, a formal reaction scheme, involving a C-protonated pyridinium ring (Scheme 1), is then proposed.

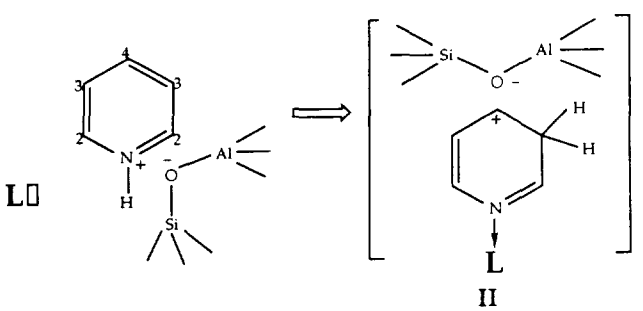

II

SCHEME 1

Since the aromatic ring is deactivated with respect to electrophilic attack in pyridinium (22), a direct shift of the proton from the N atom to a carbon atom appears unlikely. Scheme 1, if correct, should involve the desorption of pyridine from the Brønsted site, its coordination to a nearby Lewis site, a nucleophilic attack of the electron-deficient ring by a lattice oxygen (at position 2 or, more probably, 4 (23)), and, finally, protonation (at position 3). Each of these elemental steps is documented in the literature (5, 6, 9, 22–25).

According to our proposal, the formation of conjugated iminium ions, such as II in Scheme 1, would require the presence of paired Lewis/Brønsted sites. Adsorption on Lewis sites would indeed decrease the electron density at position 2 and 4, and then favour the nucleophilic attack by the negatively charged oxygen. The existence of both types of acid sites in dealuminated mazzites has been demonstrated here. This dual site could explain why the relevant infrared signals are hardly detected on the material free of extra-framework aluminium (MAZ(20–20), Fig. 5) and are the best resolved on the one containing nearly equivalent amounts of framework and extra-framework aluminium (MAZ(20–9), Fig. 4).

The transformation of a stable pyridinium ion into an iminium cation is obviously an energetically demanding process since it implies the loss of the aromatic-ring resonance energy. In other words, the sites on which the reaction proceeds must exhibit a very strong acid character. The existence of sites with very high acid strength (superacid sites) in zeolites has often been suggested (26–31). They would correspond to structural hydroxyl groups coupled with electron-deficient extra-framework aluminium species. The latter would significantly enhance the acid strength of the former by an electro-attractive effect. Such a type of site on dealuminated mazzite would readily explain our data. The question arises, however, as to why their presence was not revealed until the pyridine/zeolite surface had been subjected to high-temperature treatment, i.e., at low pyridine coverage. In addition, characterization of the acid strength of dealuminated mazzites by infrared spectroscopy of adsorbed CO, a much weaker base than pyridine, revealed that the protonic sites were indeed very strong, but the distribution of acid strengths was homogeneous (32). We believe that the reason for this behavior may be found in an evolution of the dual Lewis/Brønsted adsorption site. Both functions may be modified during the desorption of pyridine. On the one hand, Lewis sites, not present originally, can have been formed, or the strength of the existing ones may have been increased by dehydroxylation (6, 9). On the other hand, an increase of the strength of the Brønsted sites can also be invoked. Umansky *et al.* (33) have elegantly compared the behaviour of zeolites to that of superacids for which the acid strength of the protons increases with the size of the charge-compensating anion. In zeolites, the acid strength is enhanced by decreasing the aluminium content, i.e., by decreasing the charge density on the lattice which corresponds to an increase of the counteranion volume, but also by converting stable ion pairs, e.g., NH_4^+/AlO_2^- or PyH^+/AlO_2^-, into covalent Brønsted sites. If one applies this concept to the present work, it

can be argued that the charge on the lattice will decrease, and accordingly the acid strength of the structural protons will be enhanced, each time a pyridinium ion is removed from the surface as a pyridine molecule, restoring a Brønsted site. This indeed could explain why, even if very strong acid sites are present on dealuminated mazzite, iminium species are not observed after pyridine adsorption at 423 K since, at this stage, most of the structural Brønsted sites are associated with pyridinium ions, which results in high charge density on the lattice and low acid strength.

If one excepts the case of sample MAZ (20–20) outgassed at 723 K (Fig. 5c), our infrared data show that pyridine is chemisorbed in three different states, corresponding to Lewis sites, Brønsted sites, and strong Lewis/Brønsted pairs. It is noteworthy that XPS (34) and infrared (35) studies have also revealed three types of chemisorbed pyridine on MFI zeolites, attributed to Lewis sites and two kinds of Brønsted sites, weak and strong.

Finally, as regards implications for catalysis, note that considerable activity enhancement for the cracking of *n*-paraffins has been reported for MFI (36) and FAU (37) type zeolites steamed under mild conditions. Similarly, optimum activity in the hydroisomerization of light alkanes has been found for steam dealuminated mordenites (38) and mazzites (39) with framework/extra-framework aluminium ratios around 3. In all cases a synergistic effect involving Lewis (extra-framework) and Brønsted (framework) acid sites has been invoked. The generation of very strong acid centres of the type described here could account for the above observations.

CONCLUSIONS

A new interpretation is proposed for the assignment of the infrared band at 1462 cm^{-1}, which appears in the spectrum of pyridine retained on the surface of zeolites after desorption at high temperature. This band has often been attributed to a new type of coordinated pyridine. However, concomitant with the emergence of this band, other infrared signals at 2914, 2849, and 1496 cm^{-1}, and an ultraviolet band centered around 205 nm, develop. These spectral features lead us to assume that some of the adsorbed species lose their aromatic character and form conjugated iminium ions. The latter would be produced at the expense of pyridinium ions, and require the presence of a paired Lewis/Brønsted site to be stabilized. It is assumed that iminium ions form on strong acid sites which can be revealed only at low pyridine coverage, when the charge density of the lattice is low and the protonic strength high. If our hypotheses are correct, the transformation of pyridinium into iminium ions could characterize the presence of very strong sites on the surface of zeolites. Infrared spectroscopy of pyridine adsorbed at very low coverage could then help in elucidating the challenging problem of the detection of such sites on the surface of solid acid catalysts.

ACKNOWLEDGMENTS

The authors thank Drs. N. Barbouth and F. Fitoussi, Centre de Recherche ELF France, for the preparation of the samples and SNEA for financial support.

REFERENCES

1. Parry, E. P., *J. Catal.* **2,** 371 (1963).
2. Severdia, A. G., Morterra, C., and Low, M. J. D., *J. Colloid Interface Sci.* **99,** 208 (1984).
3. Bodoardo, S., Figueras, F., and Garrone, E., *J. Catal.*, in press.
4. Cannings, F. R., *J. Phys. Chem.* **72,** 4691 (1983).
5. Ghosh, A. K. and Curthoys, G., *J. Chem. Soc., Faraday Trans. I* **79,** 805 (1983).
6. Topsøe, N-Y., Pedersen, K., and Derouane, E. G., *J. Catal.* **70,** 41 (1981).
7. Mirodatos, C., and Barthomeuf, D., *J. Catal.* **57,** 136 (1979).
8. Hernandez, F., Oliver, C., Fajula, F., and Figuéras, F., *in* "Proceedings, 7th International Zeolite Conference, Tokyo, Japan, August 1986," p. 685. Kodansha Ltd., Tokyo, 1986.
9. Ghosh, A. K., and Kydd, R. A., *Zeolites* **10,** 766 (1990).
10. Jia, C., Massiani, P., and Barthomeuf, D., *J. Chem. Soc., Faraday Trans.* **89,** 3659 (1993).
11. Tanabe, K., and Hattori, H., *Chem. Lett.*, 625 (1976).
12. Takahashi, O., Yamauchi, T., Sakuhara, T., Hattori, H., and Tanabe, K., *Bull. Chem. Soc. Jpn.* **53,** 1807 (1980).
13. Fajula, F., Nicolas, S., Di Renzo, F., Gueguen, C., and Figuéras, F., *ACS Symp. Ser.* **398,** 493 (1989).
14. Di Renzo, F., Fajula, F., Barbouth, N., Schulz, Ph., and Des Courières, T., French Pat. Appl., 92 14774 (1992).
15. Massiani, P., Chauvin, B., Fajula, F., Figuéras, F., and Gueguen, C., *Appl. Catal.* **42,** 105 (1988).
16. Chauvin, B., Massiani, P., Dutartre, R., Figuréras, F., Fajula, F., and Des Courières, T., *Zeolites* **10,** 174 (1990).
17. Janin, A., Maache, M., Lavalley, J. C., Joly, J. F., Raatz, F., and Szydlowski, N., *Zeolites* **11,** 391 (1991).
18. Barnes, R. A., *in* "Pyridine and Its Derivatives" (E. Klingsberg, Ed.), Part I, p. 10. Interscience, New York, 1960.
19. Shaw, E. N., *in* "Pyridine and Its Derivatives" (E. Klingsberg, Ed.), Part II, p 32. Interscience, New York, 1960.
20. Woodward, R. B., *J. Am. Chem. Soc.* **64,** 72 (1942).
21. Scokart, P. O., and Rouxhet, P. G., *J. Chem. Soc., Faraday Trans. I* **76,** 1476 (1980).
22. Cram, D. J., and Hammond, G. S., *in* "Organic Chemistry," 2nd ed., p. 590. McGraw–Hill, New York, 1964.
23. Bennasar, M. L., Alvarez, M., Lavilla, R., Zulaica, E., and Bosch, J., *J. Org. Chem.* **55,** 1156 (1990).
24. Doddi, G., Ercolani, G., and Mencarelli, P., *J. Org. Chem.* **57,** 4431 (1992).
25. Lyle, R. E., and Gauthier, G. J., *Tetrahedron Lett.*, 4615 (1965).
26. Mirodatos, C., and Barthomeuf, D., *J. Chem. Soc., Chem. Commun.*, 39 (1981).
27. Shannon, R. D., Staley, R. H., and Auroux, A., *Zeolites* **7,** 301 (1987).
28. Garralon, G., Corma, A., and Fornes, V., *Zeolites* **9,** 84 (1989).
29. Fritz, P. O., and Lunsford, J. H., *J. Catal.* **118,** 85 (1989).
30. Sun, Y., Chu, P. J., and Lunsford, J. H., *Langmuir* **7,** 3027 (1991).

31. Chambellan, A., Chevreau, T., Khatbou, S., Marzin, M., and Lavalley, J. C., *Zeolites* **12,** 306 (1992).
32. Boulet, M., Bourgeat-Lami, E., Fajula, F., Des Courières, T., and Garrone, E., *in* "Proceedings, 9th International Zeolite Conference, Montreal, Canada, July 1992," Vol. II, p. 389. Butterworth–Heinemann, Boston, 1992.
33. Umansky, B., Engelhardt, J., and Hall, W. K., *J. Catal.* **127,** 128 (1991).
34. Borade, R., Sayari, A., Adnot, A., and Kaliaguine, S., *J. Phys. Chem.* **94,** 5989 (1990).
35. Datka, J., and Tuznik, E., *J. Catal.* **102,** 43 (1986).
36. Lago, R. M., Haag, W. O., Mikovsky, R. H., Olson, D. H., Schmidt, K. D., and Kerr, G. T., *in* "Proceedings, 7th International Zeolite Conference, Tokyo, Japan, August 1986," p. 677. Kodansha Ltd., Tokyo, 1986.
37. Beyerlein, R. A., McViker, G. B., Yacallo, L. N., and Ziemiak, J. J., *J. Phys. Chem.* **92,** 1967 (1988).
38. Corma, A., Frontela, J., Lazaro, J., and Perez, M., *Prepr.—Am. Chem. Soc., Div. Pet. Chem.* **36,** 833 (1991).
39. Fajula, F., Boulet, M., Coq, B., Rajaofanova, V., Figuéras, F., and Des Courières, T., *in* "Proceedings, 10th International Congress on Catalysis, Budapest, 1992," p. 1007. Akadémiai Kiadó, 1993.